Clinical Science (2017) **131** 2721–2735
https://doi.org/10.1042/CS20171231

PORTLAND PRESS

Research Article

DLX3 promotes bone marrow mesenchymal stem cell proliferation through H19/miR-675 axis

Na Zhao[1,2,3], Li Zeng[1], Yang Liu[1], Dong Han[1], Haochen Liu[1], Jian Xu[4], Yuxi Jiang[5], Cuiying Li[6], Tao Cai[7,8], Hailan Feng[1] and Yixiang Wang[6]

[1]Department of Prosthodontics, Peking University School and Hospital of Stomatology; [2]Department of Prosthodontics, Shanghai Stomatological Hospital; [3]Oral Biomedical Engineering Laboratory, Shanghai Stomatological Hospital, Fudan University; [4]School of Physics and Electronic Information, Henan Polytechnic University; [5]Stomatological Hospital of Yantai, Binzhou Medical University, Yantai; [6]Central Laboratory, Peking University School and Hospital of Stomatology; [7]Institute of Genomic Medicine, Wenzhou Medical University; [8]National Institute of Dental and Craniofacial Research, NIH, Bethesda, MD

Correspondence: Hailan Feng (kqfenghl@bjmu.edu.cn) and Yixiang Wang (kqwangyx@bjmu.edu.cn)

The underlying molecular mechanism of the increased bone mass phenotype in Tricho-dento-osseous (TDO) syndrome remains largely unknown. Our previous study has shown that the TDO point mutation c.533A>G, Q178R in DLX3 could increase bone density in a TDO patient and transgenic mice partially through delaying senescence in bone marrow mesenchymal stem cells (BMSCs). In the present study, we provided a new complementary explanation for TDO syndrome: the *DLX3* (Q178R) mutation increased BMSCs proliferation through H19/miR-675 axis. We found that BMSCs derived from the TDO patient (TDO-BMSCs) had stronger proliferation ability than controls by clonogenic and CCK-8 assays. Next, experiments of overexpression and knockdown of wild-type DLX3 via lentiviruses in normal BMSCs confirmed the results by showing its negative role in cell proliferation. Through validated high-throughput data, we found that the *DLX3* mutation reduced the expression of H19 and its coexpression product miR-675 in BMSCs. Function and rescue assays suggested that *DLX3*, long noncoding RNA H19, and miR-675 are negative factors in modulation of BMSCs proliferation as well as NOMO1 expression. The original higher proliferation rate and the expression of *NOMO1* in TDO-BMSCs were suppressed after H19 restoration. Collectively, it indicates that DLX3 regulates BMSCs proliferation through H19/miR-675 axis. Moreover, the increased expression of NOMO1 and decreased H19/miR-675 expression in *DLX3* (Q178R) transgenic mice, accompanying with accrual bone mass and density detected by micro-CT, further confirmed our hypothesis. In summary, we, for the first time, demonstrate that DLX3 mutation interferes with bone formation partially through H19/miR-675/NOMO1 axis in TDO syndrome.

Introduction

Tricho-Dento-Osseous syndrome (TDO; OMIM 190320) is an autosomal dominant hereditary disease comprising marked phenotypic changes in the hair, teeth, and bones. The mainly clinic features are kinky hair, thin-pitted enamel, and dentin hypoplasia, as well as abnormally thickened cortical and increased trabecular bone density of cranial and mandibular [1-4]. To date, genetic studies have found six mutations in distal-less homeobox 3 gene (*DLX3*) that is belonged to the distal-less vertebrate family (*DLX1–6*) and is known to be responsible for TDO syndrome [1-6]. As a homeodomain transcription factor, DLX3 has been found to be expressed in hair follicle cells, tooth primordium, branchial arches, developing and postnatal bones, and to participate in the process of skin, teeth and bone formation, which correlate with tissues affected in TDO syndrome [7,8].

Bone marrow mesenchymal stem cells are a population of hierarchical postnatal stem cells with multipotentials to differentiation into various cell types, such as osteoblasts, chondrocytes, and

Received: 17 July 2017
Revised: 03 September 2017
Accepted: 27 September 2017

Accepted Manuscript Online: 28 September 2017
Version of Record published: 13 November 2017

Clinical Science (2017) **131** 2721–2735
https://doi.org/10.1042/CS20171231

adipocytes [9,10]. Bone formation depends on BMSCs osteogenic potential and also BMSCs proliferation, which generates more population osteoblastic cells to perform osteogenic function. Previous studies have shown that DLX3 has a complicated role in bone formation by the evidence of *in vitro* and *in vivo* experiments [11-15]. However, whether DLX3 affects BMSCs proliferation or not still remains unknown.

Our previous studies showed that the BMSCs isolated from the mandibular of a TDO patient with a novel DLX3 mutation (c.533A>G, Q178R, named as TDO-BMSCs) demonstrated decreased osteogenic differentiation capability but increased bone mineral density in mandibular, when compared with the age- and gender-matched normal controls (named as CON-BMSCs). Obviously, the increased bone density is not contributed by the decreased osteogenic potentials of BMSCs. We have verified that the TDO point mutation Q178R in DLX3 could increase bone density in a TDO patient and transgenic mice partially through regulating senescence of bone marrow mesenchymal stem cells (BMSCs) [11]. In the epidermal cells, a previous study showed that the transgenic mice overexpressing *Dlx3* tended to be smaller, and the basal cell of the affected mice ceased to proliferation, which implies that DLX3 exerts a vital role in cell proliferation. Therefore, we suppose that DLX3 might get involved in the process of bone formation by its influence on BMSCs proliferation.

Long noncoding RNAs (lncRNAs), which are greater than 200 nucleotides without protein-coding potential, have emerged as the orchestrators of gene expression modulatory and cellular biological regulatory networks [16,17]. As one of the most well-known lncRNAs, H19 has been implicated in human genetic disorders by controlling of RNA progressing, cellular proliferation and differentiation, and disease development [18,19]. The high-throughput data analysis between TDO- and CON-BMSCs, in this report, exhibits that H19 expression is remarkably altered. Additionally, previous studies have revealed the regulatory roles of H19 in cell proliferation through direct regulator of proliferation Nodal modulator 1 protein (NOMO1), by serving as a precursor for microRNA-675 [18,19]. NOMO1 is an antagonist of Nodal signaling pathway, which is critical in regulating trophoblast cell growth. Therefore, we further presume that H19 can probably be the core factor by which DLX3 regulates cell proliferation.

To sum up, in the present study, we focus on exploring and excavating the regulatory role and associated pathway of DLX3 in proliferation with the invaluable information supplied by BMSCs from the TDO patient, and try to give an explanation of pathogenic mechanism in bone phenotype of TDO from a novel viewpoint.

Materials and methods

Cell culture and generation of transgenic mice

As described in our previous study, the present study was approved by the Ethics Committee of Peking University School and Hospital of Stomatology, and the whole methods were carried out in accordance with the relevant guidelines [20]. All animal experiments were approved by the Peking University Animal Care and Use Committee [11]. In the *in vitro* studies, the normal control BMSCs are from five different persons matched the same age and gender with the TDO patient. In all animal experiments, female transgenic mice and female wild-type littermates as controls were used. We established a sample of at least five mice per group. All details including the BMSCs identification by flow cytometry were described in our previous studies [11].

Lentivirus construction and infection

The full-length wild-type human *DLX3* (GenBank accession number, NC_000017.1) and lncRNA*H19* (GenBank accession number, NR_002196.1) cDNA were cloned into the lentivector pLVX-IRES-ZsGreen (Hanheng Chem Technology, Shanghai, China). Recombinant lentiviruses targeting *H19* (*shH19*), pre-miR-675 (miR-675-mic), miR-675 inhibitor (miR-675-inh), and the negative control were commercially obtained (Gene Pharma Company, Shanghai, China). All lentivectors contained the gene encoding green fluorescent protein. The sequences of siRNAs of human *DLX3* used to construct shDLX3 are listed in Supplementary Table S1. The sequences of siRNAs of human shH19 used to construct shH19 are listed in Supplementary Table S2. The lentiviruses were generated by Hanheng Chem Technology and Gene Pharma Company respectively.

The viruses were used to infect BMSCs. Lentiviruses (multiplicity of infection = 100) mixed with 10 μg/ml polybrene (Sigma-Aldrich, St. Louis, MO, U.S.A.) were used to infect into BMSCs cells (1×10^5cells/100 mm dish). Lentivirus infection efficiency was determined by fluorescence microscope and confirmed infection efficiency was nearly 100% (Supplementary Figure S3).

Colony-forming unit rate assay

The colony-forming unit rate assay was performed as described: briefly, 200 primary cells were plated into 100-mm culture dishes, and the medium was changed every 3 days. At 11 days postinoculation, the cells were fixed in 4%

formaldehyde and stained with 0.5% Crystal Violet for 5 min. Colonies were counted only when they contained > 50 evenly stained cells. The colony-forming unit rate was calculated as: colony-forming unit rate = colony number/plated cell number (n=200) × 100%.

Cell counting assay and population doubling time assay

Cell proliferation was assessed with the Cell Counting Kit-8 (CCK-8, Dojindo, Japan) according to the manufacturer's instruction. Briefly, 5×10^3 cells were seeded into each well of a 96-well plate in triplicate and cultured in complete medium for 10 days. Medium was changed every other day. At every other day, cells growing in three wells were cultured in a complete medium containing 10% CCK-8 for 2 h. The optical density at 450 nm was measured using an ELx808 absorbance microplate reader (BioTek, Winooski, VT, U.S.A.). As for the population doubling time (PDT) assay, PDT was calculated from the following formula: $\text{PDT} = (t - t_0) \times \log 2/\log(N_t/N_0)$. N_0 and N_t represent the cell numbers at 0 and t time points respectively.

Quantitative real-time PCR for microRNA

MicroRNA was reversely transcribed to cDNA by using a stem–loop reverse transcription primer (RiboBio, Guangzhou, China). Quantitative RT-PCR was carried out in an ABI 7500 real-time PCR system (Life Technologies Corporation). Small nuclear RNA U6 was used as an internal control. Target gene expression ($2^{-\Delta\Delta C_t}$) was normalized against endogenous U6 RNA. The miRNA quantitative PCR primers were synthesized by RiboBio Company.

Bromodeoxyuridine (BrdU) incorporation assay

Cells were cultured with bromodeoxyuridine (BrdU) incubation for 2 h. The cells were then fixed by phosphate-buffered saline (PBS) solution with 4% paraformaldehyde for 30 min. Cells were washed by PBS and treated by 0.1% Triton for 10 min. The BrdU primary antibody (Zhangshanjinqiao, Beijing, China) was then added and incubated at 4°C for one night. Later, the cells were incubated with secondary antibody at room temperature for 1 h. Then, the BrdU positive cells in each clone per microscopic field were counted.

Real-time PCR analysis

Total RNA was extracted using TRIzol (Invitrogen Life Technologies) method. Reverse-transcription and real-time PCR were performed as described in reference Zhao et al. [11]. The sequences of each primer are listed in Supplementary Tables S3 and S4.

Western blot assay

Western blot assay was used to detect the expression of proliferation-related protein expression. The detailed procedures were described as reference Zhao et al. [11]. Primary antibodies were anti-human DLX3 (Abcam), anti-NOMO1 (Cell Signaling Technology, Danvers, MA, U.S.A.), anti-Cyclin D1 (Cell Signaling Technology), anti-CDK4 (Cell Signaling Technology), and anti-GAPDH (Proteintech, Chicago, IL, U.S.A.). Results were visualized by Odyssey infrared imaging system (Odyssey LI-COR Biosciences, Lincoln, NE, U.S.A.).

Micro-CT analysis

Micro-CT analysis was used to measure bone architecture of distal femurs between 0.5 and 1.0 mm proximal to the growth plate in order to include the secondary trabecular spongiosa using Inveon micro-CT (Siemens, Munich, Germany). The parameters were set as our previous study [11]. 3D image was reconstructed by micro-CT image analysis software (Inveon Research Workplace) to visualize bone density.

Immunohistochemical analysis

The specimens were decalcified in 10% ethylenediaminetetraacetic acid (EDTA) for 1 month, and sectioned (5 μm) for staining as previously described. The slides were incubated with primary antibody against NOMO1 (Proteintech, Rosemont, IL, U.S.A.) at 4°C overnight, following incubation of the secondary antibody, the Alexa Fluor 555-conjugated anti-rabbit antibodies (Thermo Fisher Scientific Inc., Waltham, MA, U.S.A.). The image was visualized, captured, and analyzed under a Confocal Laser Scanning Microscope (Zeiss, Co., Germany).

Clinical Science (2017) **131** 2721–2735
https://doi.org/10.1042/CS20171231

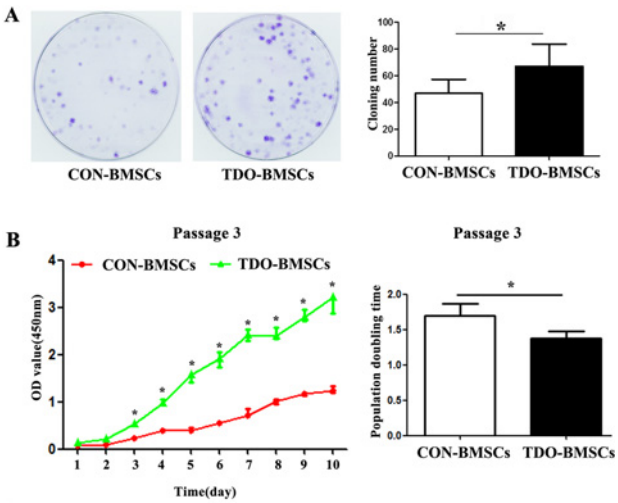

Figure 1. DLX3 mutation results in increased proliferation of BMSCs from a TDO patient

(**A**) Clonogenesis of BMSCs from the TDO patient and gender- and age-matched normal donors, as shown by Crystal Violet staining, and the statistical analysis of clonogenic results. (**B**) Proliferation rate of TDO- and CON-BMSCs at the 3rd passages. The population doubling time (PDT) of BMSCs at 3rd were significantly shorter in TDO-BMSCs than CON-BMSCs. Data were presented as the mean ± S.D. of three independent experiments; *$P<0.01$.

Statistical analysis

All data were representative of each assay repeated independently at least three times with similar results. Statistical significance was determined using the two-tailed Student's *t*-test, assuming equal variances. The χ^2 test was used to compare rates. Significance is indicated as follows:*$P<0.01$.

Results

DLX3 mutation results in an increased proliferation of BMSCs

The BMSCs used in the present study was from a typical TDO female patient with DLX3 mutation (c.533A>G; Q178R) enrolled in our previous and the present study (named as TDO-BMSCs) and the control BMSCs from donors with the same age and gender (CON-BMSCs) [5,11]. We continued our study basing on those BMSCs. The quantity and quality of BMSCs, which refers the proliferation rate and osteogenic potential of BMSCs, are the key factors in bone formation process. The increased bone formation in the TDO patient suggests that DLX3 mutation may have an intrinsic effect on the proliferation and osteogenic potential of BMSCs. Our previous studies have shown that the TDO-BMSCs exhibited a decreased osteogenic potential, which apparently could not account for the bone accrual in the TDO patient [5,11]. Therefore, we further explored the proliferation rate of the TDO-BMSCs.

Primary cells were used for colony-forming unit assay (CFU) to assess self-renewal ability of stem cells. The TDO-BMSCs generated significantly more numbers of colonies than the CON-BMSCs (Figure 1A). In addition, CCK-8 assay was used to analyze cellular proliferation at different passages. The TDO-BMSCs showed a higher proliferative rate than the CON-BMSCs (Figure 1B and Supplementary Figure S1) at the passage 3rd, 5th, and 7th respectively. Consistently, the PDT of the TDO-BMSCs was markedly shorter than that of CON-BMSCs at the passage 3rd (Figure 1B), 5th, and 7th (Supplementary Figure S1) respectively. Collectively, the TDO-BMSCs exhibited a higher proliferation rate.

DLX3 acts as a negative regulator in BMSCs proliferation

Since the *DLX3* mutation could affect the proliferation behavior of BMSCs, we then investigated the role of DLX3 in cellular proliferation through overexpression and knockdown function experiments. The recombinant lentiviruses carrying wild-type *DLX3* and *shDLX3* (selected from three *shDLX3s*, Supplementary Figure S2) expression cassettes were infected into normal BMSCs (named as wtDLX3 and shDLX3 respectively). The infection efficiency was nearly 100% detected by GFP fluorescence at 48 h (Supplementary Figure S3). Both real-time PCR and Western blot analysis showed that DLX3 was substantially increased in wtDLX3 (Figure 2A), but remarkably decreased in shDLX3 (Figure 2G), compared with control cells which were transfected with empty vector.

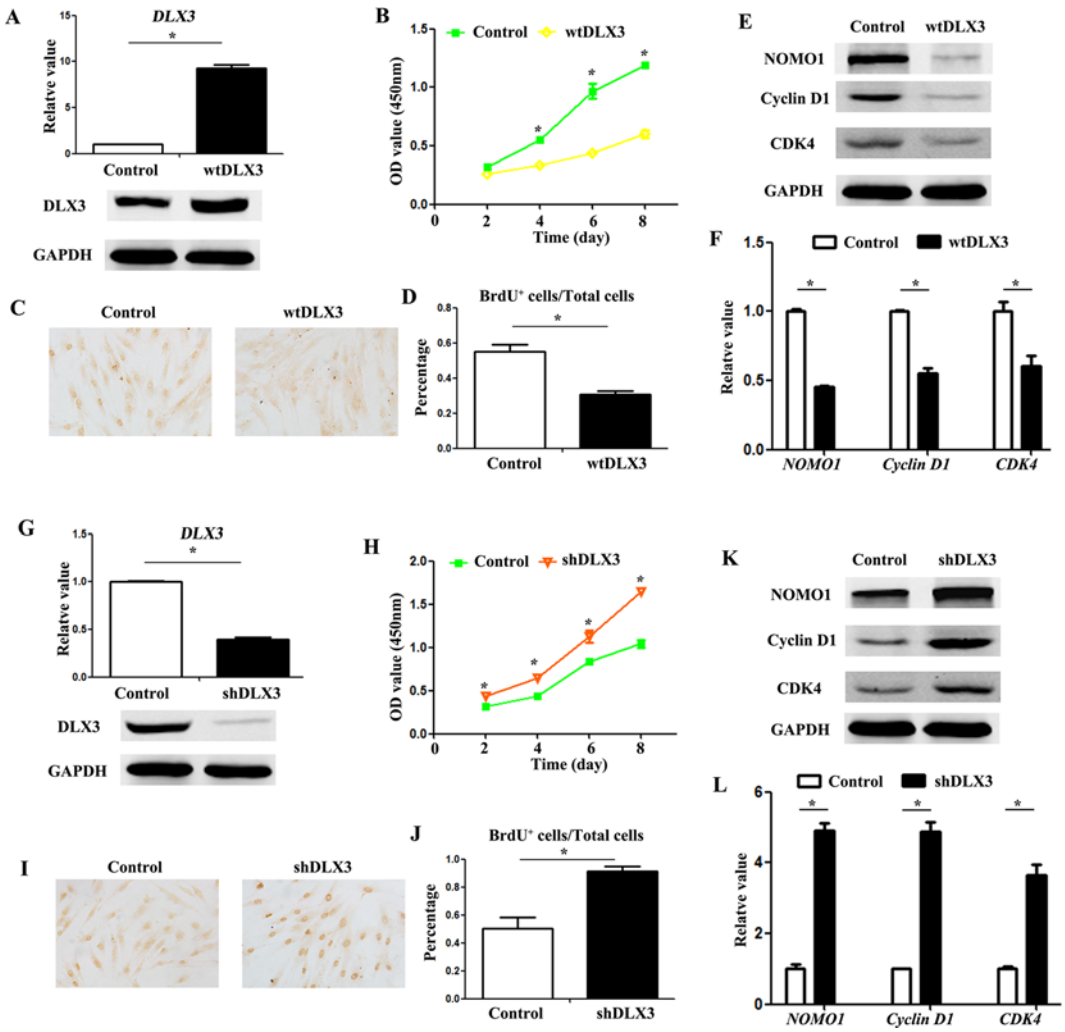

Figure 2. Overexpression of *DLX3* inhibits, whereas knockdown of *DLX3* promotes the proliferation of BMSCs

(**A**) DLX3 expression was detected by real-time PCR and Western blotting at 96 h after lentivirus infection with control and wild-type *DLX3* lentiviruses (wtDLX3). (**B**) CCK-8 assay showed that wtDLX3 overexpression inhibited BMSCs proliferation. (**C** and **D**) BrdU incorporation assay showed DLX3 overexpression cells at 48 h after infection, which was in line with CCK-8 result. (**E** and **F**) Western blotting and real-time PCR analysis of proliferation-related genes (NOMO1, Cyclin D1, and CDK4) expression in DLX3 overexpression cells at 96 h after lentivirus infection. (**G**) DLX3 was markedly deduced in BMSCs at 96 h after infection with negative control and *shDLX3* lentiviruses (shDLX3) using real-time PCR and Western blotting. (**H**) CCK-8 assay showed that DLX3 knockdown could promote BMSCs proliferation. (**I** and **G**) BrdU incorporation assay for the proliferative effect of DLX3 knockdown on BMSCs at 48 h after infection, which result was consistent with CCK-8 result. (**K** and **L**) Analyses of the proliferation-related genes (NOMO1, Cyclin D1, and CDK4) expression in DLX3 knocked down cells at 96 h after infection by Western blotting and real-time PCR. Data are presented as the mean ± S.D. of three independent experiments; *P<0.01; scale bar, 100 μm.

The CCK-8 assay showed that the proliferation rate was significantly decreased in wtDLX3 cells (Figure 2B), and highly increased in shDLX3 cells (Figure 2H). Notably, the BrdU incorporation assay exhibited that the ratio of BrdU positive cells to total cells was 32% in wtDLX3 (Figure 2C and D) and 71% in shDLX3 (Figure 2I and J), suggesting a lower proliferation rate in wtDLX3 cells and a higher rate in shDLX3.

CyclinD1, CDK4, and NOMO1 are key factors for cellular proliferation. Therefore, we examined their expression levels in the cultured cells. Real-time PCR analysis and Western blot analysis showed that NOMO1, cyclin D1, and CDK4 mRNA and protein expression were significantly decreased in wtDLX3-transfected cells (Figure 2E and F), but notably increased in shDLX3-transfected cells (Figure 2K and L).

Clinical Science (2017) **131** 2721–2735
https://doi.org/10.1042/CS20171231

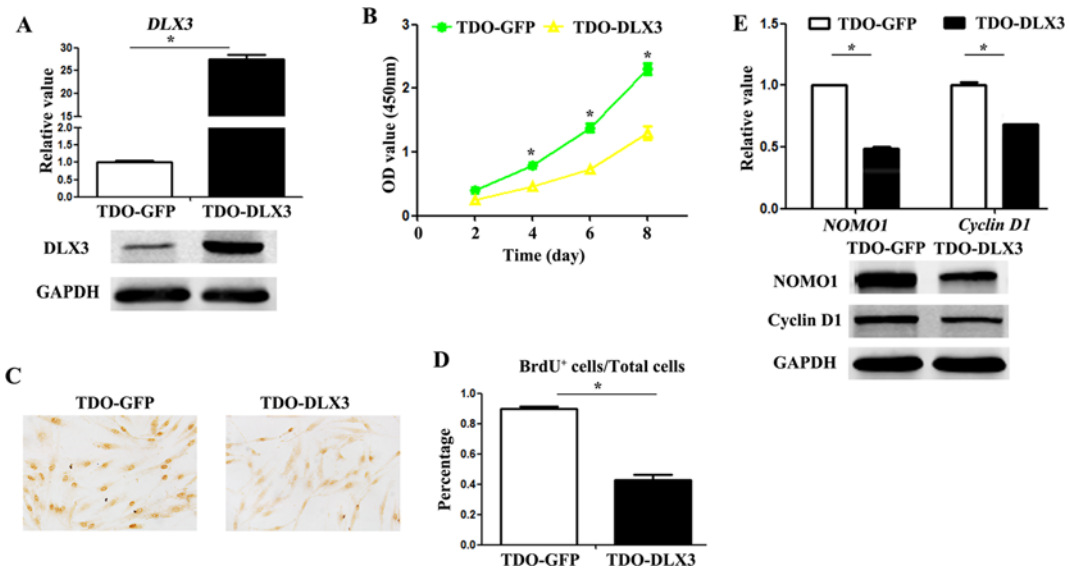

Figure 3. The restoration of wild-type DLX3 expression in TDO-BMSCs inhibits BMSCs proliferation

(**A**) Overexpression of DLX3 in TDO-BMSCs. Wild-type GFP-DLX3 was highly expressed in TDO-BMSCs as determined by real-time PCR and Western blotting analysis. Glycerol dehyde-phosphate dehydrogenase (GAPDH) was used as an internal control. (**B**) Overexpression of DLX3 inhibited TDO-BMSCs proliferation. CCK-8 assay of wild-type DLX3 overexpressed TDO-BMSCs (named as TDO-DLX3). (**C** and **D**) BrdU incorporation assay of wild-type DLX3 overexpressed TDO-BMSCs at 48 h after infection. (**E**) Real-time PCR and Western blotting analysis of proliferation-related genes expression (NOMO1 and Cyclin D1) in wild-type DLX3 overexpressed TDO-BMSCs at 96 h after infection. Data were presented as the mean ± S.D. of three independent experiments; $^{*}P<0.01$.

Collectively, overexpression of *DLX3* inhibited proliferation of BMSCs, whereas knockdown of *DLX3* resulted in the proliferation of BMSCs. These results indicate that DLX3 acts as a negative regulator in BMSCs proliferation.

Restoration of wild-type DLX3 in TDO-BMSCs inhibits BMSCs proliferation

Since the function studies have demonstrated that DLX3 as a negative regulator in BMSCs proliferation, we thus performed the rescue experiments to further confirm those results.

It is worth mentioning that the DLX3 expression was lower in TDO-BMSCs when compared with CON-BMSCs [5,11]. Therefore, we first restored the wild-type DLX3 lentiviruses in TDO-BMSCs (named as TDO-DLX3). The TDO-BMSCs infected with control GFP lentiviruses were served as a control and named as TDO-GFP. DLX3 expression was significantly enhanced in TDO-DLX3 as determined by real-time PCR and Western blot analyses (Figure 3A). The CCK-8 assay demonstrated that TDO-DLX3 exhibited a lower proliferation rate, which indicated that the high proliferation rate in TDO-BMSCs was inhibited after DLX3 expression was restored (Figure 3B). Meanwhile, the number of BrdU positive cells was also reduced in TDO-DLX3 (Figure 3C and D). Additionally, the mRNA and protein expression of NOMO1 and Cyclin D1 were depressed in TDO-DLX3 detected by real-time PCR and Western blot analysis (Figure 3E).

Collectively, the high proliferation rate was inhibited by wild-type DLX3 restoration, which confirmed a negative effect of DLX3 on BMSCs proliferation.

H19/miR-675 is suppressed in TDO-BMSCs with DLX3 mutation

Both the function study and the rescue study have proved that DLX3 could inhibit BMSCs proliferation. The underlying mechanism remains unclear. We assumed that noncoding RNAs might be involved in the process, and thus tried to identify differently expressed molecules between TDO- and CON-BMSCs with long noncoding RNA chips. Among the targets validated in BMSCs, H19 expression underwent the greatest change (data not shown). Real-time PCR analysis showed the expression of H19 and its precursor of miR-675 were dramatically suppressed in TDO-BMSCs, which is consistent with the high-throughput analysis (Figure 4A).

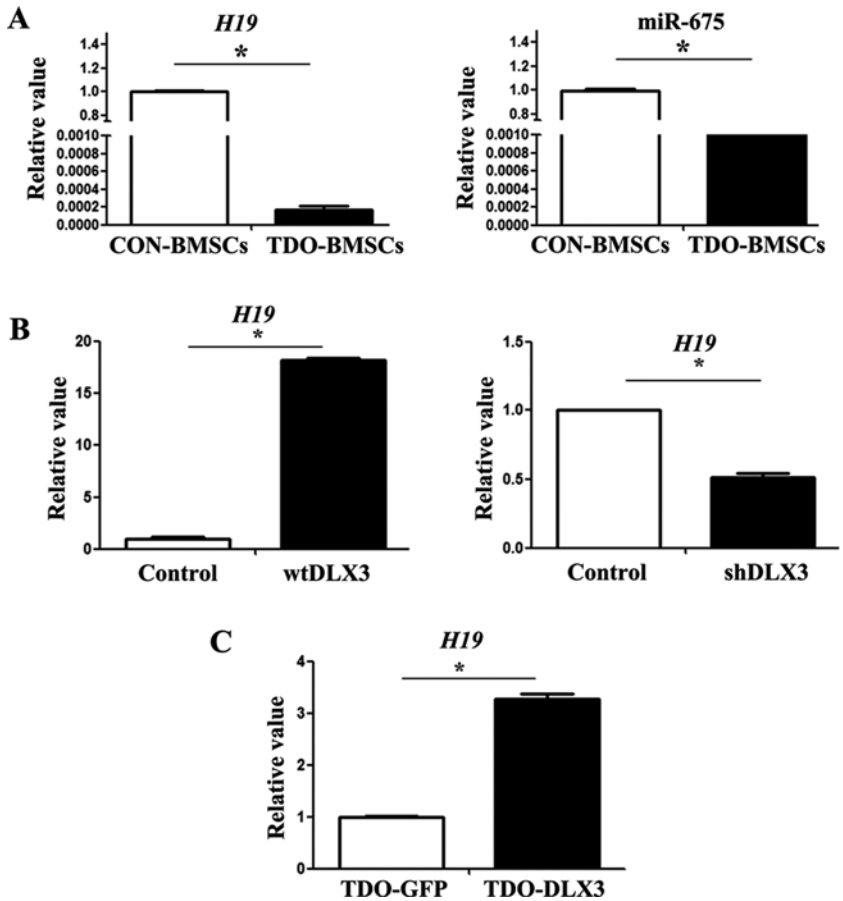

Figure 4. H19/miR-675 expression is suppressed in TDO-BMSCs with DLX3 mutation

(**A**) Gene expression profile revealed that H19 and miR-675 were significantly reduced in TDO-BMSCs. H19 and miR-675 expression were determined by real-time PCR. GAPDH and U6 were used as corresponding internal controls. (**B**) Real-time PCR analysis of H19 expression in normal BMSCs infected with wtDLX3 and shDLX3 lentiviruses respectively at 96 h postinfection. (**C**) Real-time PCR analysis of H19 expression in TDO-BMSCs infected with wtDLX3 lentiviruses at 96 h after infection. Data were presented as the mean ± S.D. of three independent experiments; *$P<0.01$.

Real-time PCR analysis was used to detect H19 expression which was promoted in normal BMSCs with wild-type DLX3 infection and inhibited in normal BMSCs with shDLX3 infection after 96 h (Figure 4B). Additionally, H19 was highly increased in the cells of TDO-BMSCs after DLX3 overexpression (Figure 4C). It clearly suggests that abundant DLX3 can promote H19 expression then leading to decelerate cell proliferation rate.

H19/miR-675 negatively regulates BMSCs proliferation

Previous studies reported that H19 inhibits cell proliferation via miR-675 in various cell lines, such as ES cells, TS cells, MEF cells, and C2C12 cells [5,11]. Therefore, we re-examined the role of H19 and miR-675 in proliferation of BMSCs. Real-time PCR analysis showed that H19 was highly expressed in BMSCs by wild-type *H19* lentiviruses infection (named as H19; Figure 5A) and was significantly knocked down in BMSCs by *shH19* (selected from two *shH19s*, Supplementary Figure S2) lentiviruses infection (named as shH19; Figure 5C). CCK-8 assay showed that the BMSCs proliferation rate was lower in H19 cells (Figure 5B) but higher in shH19 cells (Figure 5D), suggesting that H19 negatively regulates BMSCs proliferation. Consistently, the miR-675 exhibited the same function (Figure 5E and F) as H19 gene in BMSCs. The real-time PCR and Western blot analysis showed that miR-675 and its target gene NOMO1 were significantly enhanced in BMSCs transfected with lentiviruses carrying miR-675 mimics (named as miR-675-mic) and significantly declined in BMSCs transfected with lentiviruses carrying miR-675 inhibitor (miR-675-inh) (Figure 5E). The CCK-8 assay demonstrated that the BMSCs proliferation rate was greatly decreased in miR-675-mic, but remarkably increased in miR-675-inh (Figure 5F).

Clinical Science (2017) **131** 2721–2735
https://doi.org/10.1042/CS20171231

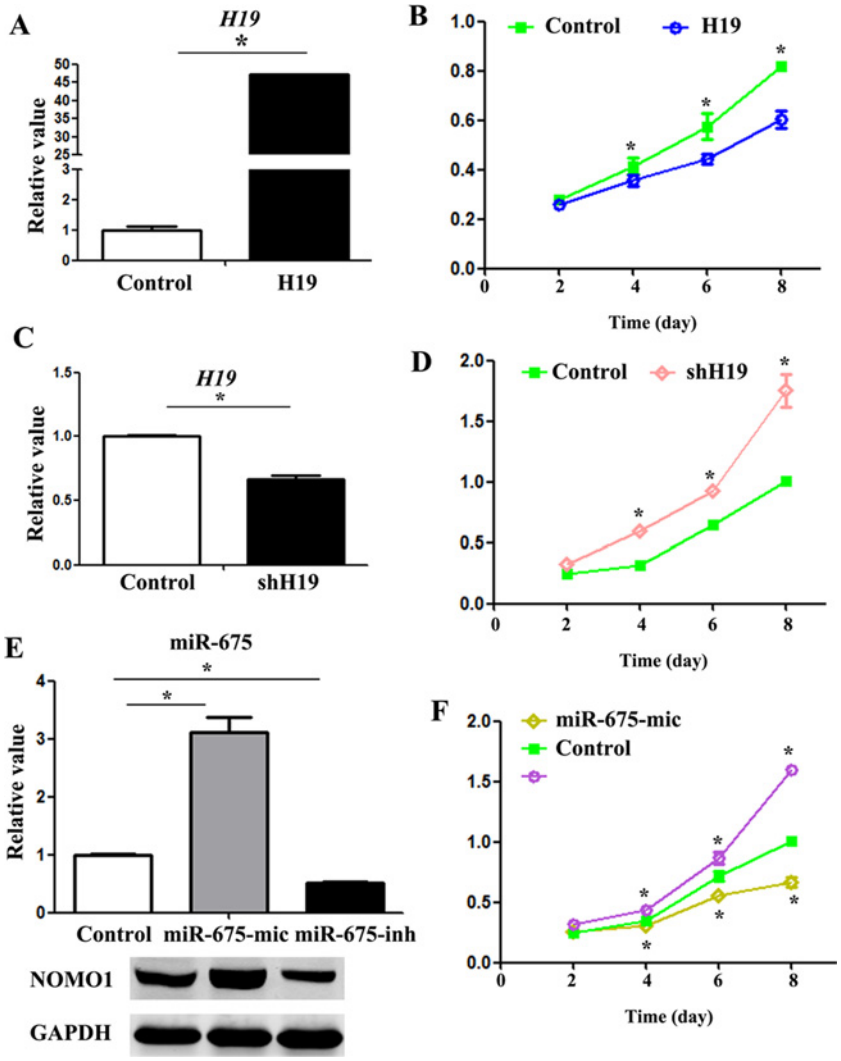

Figure 5. H19/miR-675 negatively regulates BMSCs proliferation

(**A**) Overexpression of H19 decreased BMSCs proliferation. Real-time PCR analysis showed that *H19* was highly overexpressed in BMSCs. (**B**) The proliferation rate of wild-type H19 overexpression in BMSCs was analyzed by CCK-8 assay. (**C**) Knockdown of H19 increased BMSCs proliferation. Real-time PCR analysis showed that *H19* was significantly reduced in BMSCs. (**D**) CCK-8 assay was used for analysis of proliferation rate in shH19 knocked down cells. (**E**) miR-675 inhibited BMSCs proliferation. Real-time PCR analysis and Western blot analysis showed that miR-675 expression and its target (NOMO1) were significantly increased in BMSCs transfected with lentiviruses carrying miR-675 mimics (miR-675-mic) and decreased in BMSCs transfected with lentiviruses carrying miR-675 inhibitor (miR-675-inh). (**F**) CCK-8 assay was used for analysis of proliferation rate in miR-675 overexpression and knocked down cells. Data were presented as the mean ± S.D. of three independent experiments; $^{*}P<0.01$.

Taken together, we have proved that both DLX3 and H19/miR-675 negatively regulate BMSCs proliferation. Interestingly, the TDO-BMSCs with a high proliferation rate are accompanying with lower DLX3 and H19/miR-675 expression. Therefore, our findings revealed that DLX3 regulates BMSCs proliferation through H19/miR-675.

Restoration of H19/miR-675 in TDO-BMSCs inhibits cell proliferation

To further examine whether H19/miR-675 on BMSCs can "rescue" the proliferative ability in TDO-BMSCs, we restored H19 expression in TDO-BMSCs, which exhibited lower H19 expression. Like the rescue experiments of DLX3 restoration in TDO-BMSCs, real-time PCR analysis showed that H19 expression was significantly augmented in TDO-BMSCs infected with H19 lentiviruses (named as TDO-H19) (Figure 6A), compared with the control cells

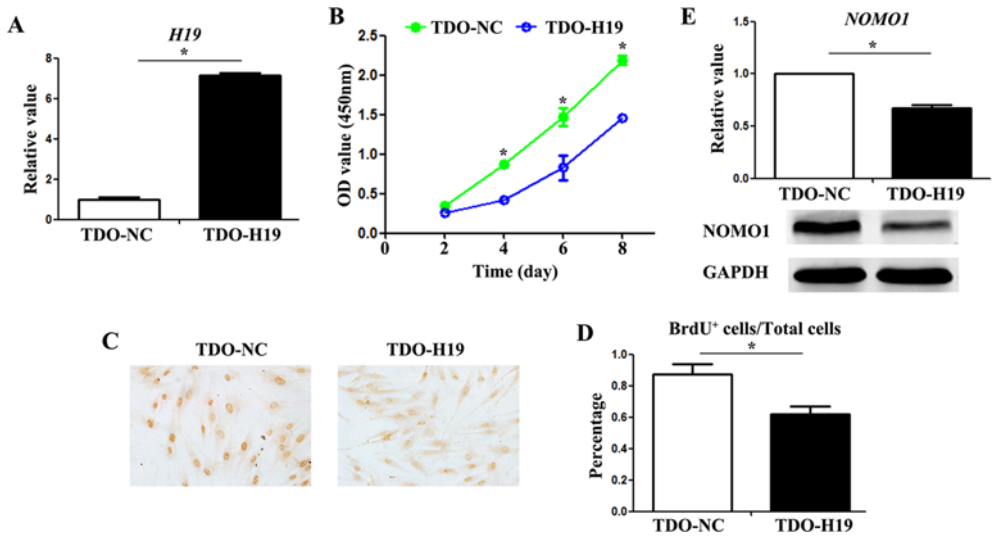

Figure 6. The restoration of H19 in TDO-BMSCs inhibits BMSCs proliferation

(**A**) Overexpression of H19 in TDO-BMSCs. *H19* was highly expressed in TDO-BMSCs as determined by real-time PCR. GAPDH was an internal control. (**B**) Overexpression of H19 inhibited TDO-BMSCs proliferation. CCK-8 assay measured proliferation rate of the wild-type H19 expression in TDO-BMSCs (named as TDO-H19). (**C** and **D**) BrdU incorporation assay measured proliferation rate of TDO-H19 cells at 48 h after infection. (**E**) Real-time PCR and Western blotting analysis of the proliferation-related gene expression (NOMO1) in H19 overexpressed TDO-BMSCs at 96 h after infection. Data were presented as the mean ± S.D. of three independent experiments; $^{*}P<0.01$.

transfected with empty lentiviruses (named as TDO-NC). Moreover, CCK-8 assay demonstrated that TDO-H19 exhibited a lower proliferation rate, indicating that the proliferation rate in TDO-BMSCs was inhibited by restoration of H19 expression (Figure 6B). The number of BrdU positive cells was also decreased in TDO-H19 (Figure 6C and D).

Additionally, mRNA expression of *NOMO1* was depressed in TDO-H19 detected by real-time PCR, which further confirmed by Western blot analysis (Figure 6E).

Collectively, the inhibitory role of H19 on the TDO-BMSCs proliferation indicates that H19 could reverse the effect of DLX3 (Q178R) on TDO-BMSCs proliferation, consistent with the decreased H19/miR-675 expression in TDO-BMSCs due to the *DLX3* mutation.

DLX3 (Q178R) mutant increases bone mass and BMSCs proliferation *in vivo*

Since the *in vitro* study proved the regulatory role of DLX3 in BMSCs proliferation through H19/miR-675, we further verified this result *in vivo* using transgenic mice expressing the *DLX3* mutation (named as DLX3 (Q178R)-Tg mice). Since our previous study have demonstrated that DLX3 (Q178R) was highly expressed in femur and tibia bone of DLX3 (Q178R)-Tg mice [5,11], we here further confirmed DLX3 in different locations of femur bones (Supplementary Figure S4). The immunostaining shows that the number of DLX3 positive cells is much higher in the location of the cortical bone body and head of femurs as well as the secondary trabecular spongiosa of the distal femurs in 6-month-old DLX3 (Q178R)-Tg mice than those in gender- and age-matched WT mice (Supplementary Figure S4). It not only does reveal that DLX3 is expressed in the different areas of bone tissues, but also suggests that the transgenic mice are successfully built. To determine the difference of bone formation, we then quantified several structural parameters of femurs in 6-month-old male mice with micro-CT analysis. Although no significant difference was observed in the length of femurs, 3D reconstruction and sagittal femur micro-CT analysis showed an increased mass and length of the trabecular bone area that extended into the diaphysis area of the DLX3(Q178R)-Tg mice (Figure 7A). The quantified data revealed an increased trabecular bone mineral density, bone volume, thickness, and number of trabeculae in DLX3(Q178R)-Tg mice. The increased number of trabeculae and connectivity was complemented by decreased trabecular spacing (Figure 7B). These results indicated that DLX3(Q178R)-Tg osteoprogenitors formed more trabeculae that extended deeper in the medullary cavity.

Clinical Science (2017) **131** 2721–2735
https://doi.org/10.1042/CS20171231

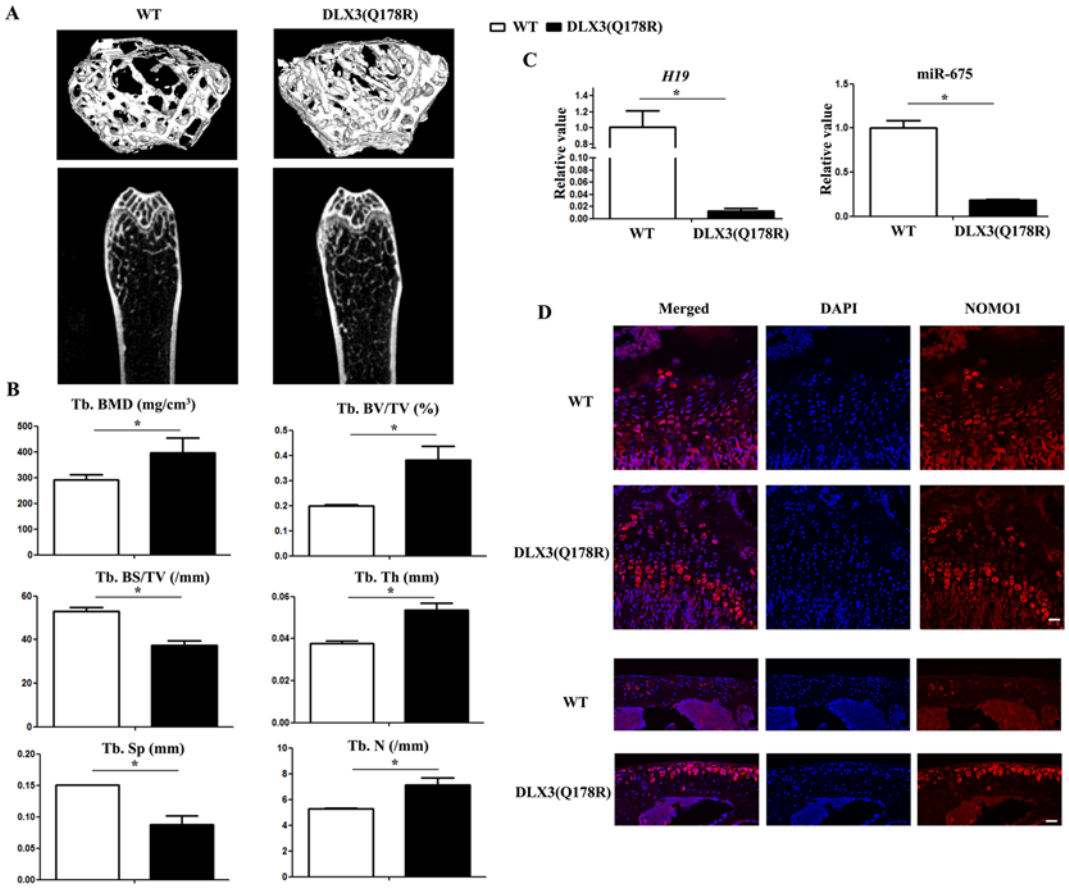

Figure 7. DLX3 (Q178R) increases bone mass and proliferation *in vivo*

(**A** and **B**) Micro-CT analysis: 3D trabecular reconstructions of distal femoral metaphysis regions from 6-month-old WT and gender- and age-matched DLX3(Q178R)-Tg mice (A). (B) Quantitative analysis: trabecular bone mineral density (Tb. BMD); trabecular bone volume/total volume (Tb. BV/TV); trabecular bone surface area/bone volume (Tb. BS/BV); trabecular thickness (Tb. Th); trabecular number (Tb. N); trabecular spacing (Tb. Sp). (**C**) H19 and miR-675 expression were significantly reduced in DLX3 (Q178R)-Tg mice. Expression *H19* and miR-675 were determined by real-time PCR. GAPDH and U6 were used as internal controls respectively. (**D**) Immunostaining showed that NOMO1 was expressed in the location surrounding with trabecular and cortical bones from 6-month-old WT and DLX3 (Q178R)-Tg mice; scale bars, 100 μm.

Immunostaining showed that primary spongiosa trabeculae (region in close proximity to the growth plate) and cortical bones were densely lined with NOMO1-positive cells, supporting that the increase in bone formation resulting from increased osteoblast proliferation (Figure 7D). Consistently, H19 and miR-675 expression were remarkably decreased in DLX3 (Q178R)-Tg mice (Figure 7C). Our study further confirmed the reduced H19 and miR-675 expression due to DLX3 (Q178R) mutation were responsible for the increased proliferation in DLX3 (Q178R)-Tg mice as well as in the TDO patient.

Discussion

Genetic studies of human with inherited disorders of skeletal development have been considered the most prestigious method to lead us to identify novel genes and pathways involving bone formation [21]. The hair, teeth, and bone defects in TDO patients, caused by single mutation of DLX3, have tremendously increased our understanding of normal as well as abnormal development of these tissues and of the regulatory roles of transcription factor DLX3 in various aspects [3,8,22]. Our previous studies have revealed DLX3 novel effects on osteogenic differentiation and senescence through experiments with BMSCs from mandibular of the TDO patient [11]. Subsequently, in the present study, we shed new light of DLX3 function on BMSCs proliferation with the precious cells to elaborate the pathology mechanism of osseous changes in the TDO patient.

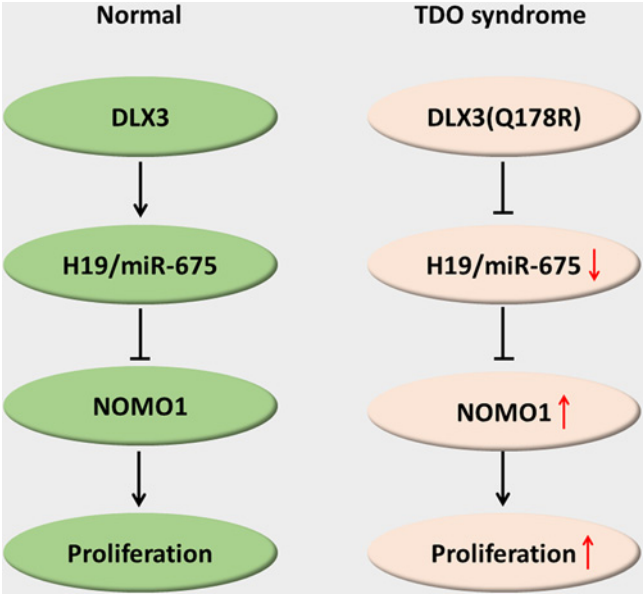

Figure 8. Schematic diagram: DLX3 regulates BMSCs proliferation through H19/miR-675/NOMO1 axis

Studies concerning DLX3 effects on proliferation have showed that cell growth and proliferation were suppressed with DLX3 reinstatement in cutaneous squamous cell carcinoma or basal epidermal cells, suggesting that DLX3 overexpression suppresses epidermal cell proliferation [23,24]. Consistently, in our previous study, not only the TDO-BMSCs at passage 9 stay relatively at younger state, but also does its number aggravate faster than that of CON-BMSCs with the same condition [11]. Therefore, it is reasonable to infer that not merely BMSCs cellular senescence but also proliferation rate is altered by DLX3 mutation in the TDO patient. In our present study, comparative experiments reveal that TDO-BMSCs lead a character with stronger self-renewal capability and faster proliferation rate. Furthermore, the gain- and loss-of-function study of DLX3 in normal BMSCs here showed that DLX3 overexpression inhibits BMSCs proliferation while knockdown of DLX3 promotes BMSCs proliferation. Besides, the restoration of DLX3 expression in TDO-BMSCs decreased the high proliferation rate due to the DLX3 mutation. Collectively, all the evidence are in accordance with previous studies by showing DLX3 as a negative regulator in BMSCs proliferation. Additionally, the higher proliferation rate caused by *DLX3* mutation was further confirmed by a higher expression level of NOMO1 and the increased mass and length of the trabecular bone area that extended into the diaphysis tissue of DLX3 (Q178R)-Tg mice.

The dramatic expression difference of long noncoding RNA H19 between TDO- and CON-BMSCs arouses our interesting for its regulatory role in cell proliferation. H19 is one of the most abundant and conserved noncoding transcripts in mammalian development, and has been demonstrated to inhibit proliferation of various cells. Herein, our gain- and loss-of-function study of H19 and miR-675 in normal BMSCs confirm their negative effects on proliferation of BMSCs. Regarding of the proliferation-related genes, Cyclin D1 and Cyclin-dependent kinase 4 (CDK4) are important regulators of cell cycle. Cyclin D1 overexpression induces cell growth and transformation and tumorigenesis by shortening cell cycle G1 phase and thus promoting entry into S phase. CDK4 takes a significant part in the G1/S transition of the cell cycle [25-27]. NOMO1, as an antagonist of Nodal signaling pathway participating in trophoblast cell growth regulation, is considered as an important direct regulator in cell proliferation. Among them, NOMO1 catches our attention for its connection with long noncoding RNA H19. Previous studies have revealed that H19 is a reservoir of miR-675 which negatively regulates NOMO1 through directly binding to its 3′-UTR [28]. According to the suppressed expression in TDO-BMSCs (along with DLX3 lower expression), H19 expression was also increased in normal BMSCs or TDO-BMSCs with DLX3 overexpression, but decreased in normal BMSCs with sh*DLX3* knockdown. It suggests that DLX3 and H19 share the same effect on proliferation, and H19 expression is regulated by DLX3 presentation or absence. What's more, after restoration of H19 expression in TDO-BMSCs, the declined proliferation rate and lower expression of NOMO1 infer that redundant H19 is able to play its negative regulatory factor on proliferation by disrupting and blocking the function of mutant DLX3 (Q178R). In addition, the bone tissue of DLX3 (Q178R)-Tg mice also exhibited lower expression of H19 and miR-675, but higher NOMO1 expression. Thereby, this idea develops further that DLX3 negatively regulates BMSCs proliferation by H19/miR-675,

Clinical Science (2017) **131** 2721–2735
https://doi.org/10.1042/CS20171231

which negatively regulates NOMO1. Whereas regarding whether H19 regulates DLX3 in the feedback way, future studies are needed to follow up.

To determine the role of DLX3 (Q178R) during bone formation, we analyzed in detail the *DLX3* (Q178R) expression and bone mass in DLX3 (Q178R)-Tg mice. With respect to the osseous changes of transgenic mice driven by keratin 14 (K14) promoter, previous study has displayed the evidence of bone loss in a mouse line with Smad2 overexpression driven by K14 promoter [29]. Consistent with this view, our pervious study has demonstrated that DLX3 (Q178R) mRNA and protein expression were highly enhanced in DLX3 (Q178R)-Tg mice [11]. Accordingly, immunohistochemical analysis showed not only that the DLX3 positive cells were detected in the cortical bone body and head of femurs as well as the secondary trabecular spongiosa of the distal femurs in WT and DLX3 (Q178R)-Tg mice, but also higher number in DLX3 (Q178R)-Tg mice (Supplementary Figure S4). As a consequence, the transgenic mice were successfully built. Then the second question comes. How do the data match the effect of DLX3 in the TDO patient to DLX3 (Q178R)-Tg mice? In the TDO patient, even though the DLX3 expression was lower, yet the DLX3 (Q178R) expression was higher when compared with the wild-type DLX3. Identically, the DLX3 (Q178R) was much more highly overexpressed in DLX3 (Q178R)-Tg mice than WT mice. In this view, the TDO patient and DLX3 (Q178R)-Tg mice share the same pattern of DLX3 (Q178R) expression resulting in higher proliferation rate and accrual bone mass. While concerning the molecular biology mechanism, it is currently unclear whether DLX3 (Q178R) is unstable or not and how DLX3 (Q178R) acted with wild-type DLX3. A more complete knowledge of the 3D spatial structure of DLX3 protein and its functional manner may be important for identification of its function in various tissues and TDO syndromes.

Proper proliferation and differentiation of BMSCs are essential for maintenance of bone formation. After reviewing previous studies, we found that DLX3 has a complex role in bone formation because of triggering a regulatory network to keep the maintenance of bone homeostasis (reviewed in Zhao et al. [11]). Our previous study demonstrated that this DLX3 mutation (Q178R) decreased osteogenesis in TDO-BMSCs, and in the pre-osteoblastic MC3T3-E1 cells with DLX3 (Q178R) overexpressed, as well as in the DLX3 (Q178R)-Tg mice [11]. Interestingly, the expression of H19 and miR-675 in TDO-BMSCs were dramatically lower. According to a previous study, H19 and miR-675 are able to promote osteoblastic differentiation via TGF-β1/Smad3/HDAC signaling pathway [30]. Therefore, it is extremely possible that the decreased osteoblast differentiation potential is caused by the lack of H19/miR-675 expression. With a deeper understanding of these issues, these results indicate that DLX3 regulates osteogenesis partially through H19/miR-675. However, the underlying mechanism needs to be investigated in the future study.

Consistently with the manifestation of the TDO patient, the DLX3 (Q178R)-Tg mice shared the same features in bone. The bone mineral density is increased but accompanying with decreased osteoblast differentiation potential. However, the TDO-BMSCs and DLX3 (Q178R)-Tg mice exhibited a delayed senescence and increased proliferation rate, which could prolong the BMSCs lifespan and produce more BMSCs to generate more bone mass [30]. Previous studies also demonstrated that the proliferation rate and self-renewal ability were enhanced when cellular senescence was jeopardized. In accordance with this, our data showed that TDO-BMSCs performed stronger self-renewal ability in the present study.

LncRNAs H19 is well known as one of the most important imprinted gene, which plays an important role in fetal development and growth control through epigenetic regulation, and is associated with various kinds of tumor and human genetic diseases, such as Beckwith–Wiedemann Syndrome and Silver–Russell Syndrome caused by alteration of methylation status in H19 gene locus [31-33]. Moreover, various tumors were arisen by the aberrant H19 expression owing to specific sites of methylation [34,35]. Furthermore, a recent study comparing microRNA expression and methylation status between patients with chronic obstructive pulmonary disease (COPD) and normal people pointed that the increased expression of H19/miR-675 resulted from DNA methylation makes an important contribution to the low fat-free mass index in patients with COPD [36]. In our study, to excavate underlying mechanisms that may attribute to the susceptibility to a high bone mass, we investigated long noncoding RNA expression, methylation status, and relative transcriptomic expression from BMSCs between the TDO patient and normal controls, which revealed that H19 was highly methylated and suppressively expressed in TDO-BMSCs. These data provide the evidence that suggests the possibility of DNA methylation involving in H19 expression regulation in TDO syndrome. However, it must be tested further how DLX3 influence the methylation status of H19. DNA methylation can be modified through a number of mechanisms including the introduction of DNA methyltransferases (DNMT1, DNMT3A, and DNMT3B) expression. Given these facts, it is tempting to postulate that DNA methyltransferases might be modulated in response to DLX3 mutation finally resulting in the alteration of H19 methylation and expression. Whereas additional experiments are needed to confirm this speculation in the future studies.

Conclusively, our findings in the rare human genetic disease unravels a novel mechanism of DLX3 involving the proliferation regulation through H19/miR-675, and provides an explanation for the increased bone formation in TDO

syndrome. In particular, we demonstrated that DLX3 mutation reduced H19/miR-675 expression, thereby resulting in repressive effects of H19/miR-675 on cell proliferation through their negative effects on NOMO1. Mechanistically, the increased bone mass is on account of the increased cell proliferation in the TDO-BMSCs, which compensates the decreased osteogenic potential by increasing the number of BMSCs. On the basis of these findings, we propose that the mechanism illustrated in Figure 8 shows that DLX3 has a negative regulatory role in BMSCs proliferation through regulation of the noncoding H19/miR-675/NOMO1 axis. To our knowledge, this represents the first case in which the decreased H19/miR-675 expression on account of DLX3 mutation is associated with the higher proliferation rate of BMSCs in TDO patient. The discovery not only deepens our understanding of DLX3 and H19 effect on proliferation, but also broadens their roles in bone formation, which might open up new avenues for future investigations of being target genes in the application of bone regeneration.

Clinical perspectives

- Bone formation is dependent not only on the activity of individual osteoblasts but also on the number of osteoblastic cells, which is determined by proliferation. Our previous study have showed that DLX3 (Q178R) decreased osteogenic potential of BMSCs, which apparently could not account for the bone accrual in the TDO patient or DLX3 (Q178R)-Tg mice. Therefore, we investigated DLX3 effect on proliferation of BMSCs in the present study.

- With the previous experimental materials isolated from TDO patient, we herein offer novel insight into DLX3 function on proliferation through long noncoding RNA H19. Our findings demonstrated that the DLX3 mutation reduced H19/miR-675 expression, thereby resulting in a repressive effect of the dysregulated NOMO1 on cell proliferation in the TDO patient. As for the underlying mechanism of TDO syndrome, our evidence suggested that the increased bone mass was on account of the increased cell proliferation in the TDO-BMSCs compensating the decreased osteogenic potential by increasing the number of BMSCs.

- Importantly, we unravel long noncoding RNA mechanism for the control of human adult stem cell proliferation through studying a rare genetic disease. The discovery deepens our understanding of DLX3 and H19 effect on proliferation and bone formation, which might open the possibility of being target genes in the application of bone regeneration.

Acknowledgments

The authors are grateful to the TDO patient and the normal healthy donors and for participating in the present study.

Author Contribution

N.Z. performed the measurement of all biomarkers, analyzed the data, created figures, and drafted the manuscript. L.Z., Y.L., D.H., H.L., and Y.J. carried out sample preparation. J.X. assisted in figures creating. C.L. and T.C. assisted in manuscript revising. H.F. and Y.W. designed the study, supervised the experiments, data acquisition, and writing of article.

Competing Interests

The authors declare that there are no competing interests associated with the manuscript.

Funding

This work was supported by grants from the National Natural Science Foundation of China [grant numbers 81570961 and81772873]; the Natural Science Foundation of Beijing Municipality [grant number 7092113]; Beijing Natural Science Foundation [grant number 7172240]; the National Key Health Research Project Foundation of China during the 11th Five-Year Plan Period [grant number 2006BAI05A07]; and the Capital Medical Developing Foundation [grant number 2007-1005].

Clinical Science (2017) **131** 2721–2735
https://doi.org/10.1042/CS20171231

Abbreviations

BMSC, bone marrow-derived mesenchymal stem cell; BrdU, bromodeoxyuridine; CCK-8, Cell Counting Kit-8; CDK4, cyclin-dependent kinase 4; *DLX3*, distal-less homeobox 3 gene; GAPDH, glycerol dehyde-phosphate dehydrogenase; LncRNAs, long noncoding RNA; NOMO1, nodal modulator 1 protein; PDT, population doubling time; TDO, tricho-dento-osseous syndrome.

References

1 Nieminen, P., Lukinmaa, P.L., Alapulli, H., Methuen, M., Suojarvi, T., Kivirikko, S. et al. (2011) DLX3 homeodomain mutations cause tricho-dento-osseous syndrome with novel phenotypes. *Cells Tissues Organs* **194**, 49–59
2 Mayer, D.E., Baal, C., Litschauer-Poursadrollah, M., Hemmer, W. and Jarisch, R. (2010) Uncombable hair and atopic dermatitis in a case of trichodento-osseous syndrome. *J. Dtsch. Dermatol. Ges.* **8**, 102–104
3 Price, J.A., Bowden, D.W., Wright, J.T., Pettenati, M.J. and Hart, T.C. (1998) Identification of a mutation in DLX3 associated with tricho-dento-osseous (TDO) syndrome. *Hum. Mol. Genet.* **7**, 563–569
4 Lichtenstein, J., Warson, R., Jorgenson, R., Dorst, J.P. and McKusick, V.A. (1972) The tricho-dento-osseous (TDO) syndrome. *Am. J. Hum. Genet.* **24**, 569–582
5 Li, Y., Han, D., Zhang, H., Liu, H., Wong, S., Zhao, N. et al. (2015) Morphological analyses and a novel de novo DLX3 mutation associated with tricho-dento-osseous syndrome in a Chinese family. *Eur. J. Oral Sci.* **123**, 228–234
6 Lee, S.K., Lee, Z.H., Lee, S.J., Ahn, B.D., Kim, Y.J., Lee, S.H. et al. (2008) DLX3 mutation in a new family and its phenotypic variations. *J. Dent. Res.* **87**, 354–357
7 Beanan, M.J. and Sargent, T.D. (2000) Regulation and function of Dlx3 in vertebrate development. *Dev. Dyn.* **218**, 545–553
8 Feledy, J.A., Morasso, M.I., Jang, S.I. and Sargent, T.D. (1999) Transcriptional activation by the homeodomain protein distal-less 3. *Nucleic Acids Res.* **27**, 764–770
9 Cohen, S.M., Bronner, G., Kuttner, F., Jurgens, G. and Jackle, H. (1989) Distal-less encodes a homoeodomain protein required for limb development in Drosophila. *Nature* **338**, 432–434
10 Owen, M. and Friedenstein, A.J. (1988) Stromal stem cells: marrow-derived osteogenic precursors. *Ciba Found. Symp.* **136**, 42–60
11 Zhao, N., Han, D., Liu, H., Li, Y., Wong, S.W., Cao, Z. et al. (2016) Senescence: novel insight into DLX3 mutations leading to enhanced bone formation in Tricho-Dento-Osseous syndrome. *Sci. Rep.* **6**, 38680
12 Isaac, J., Erthal, J., Gordon, J., Duverger, O., Sun, H.W., Lichtler, A.C. et al. (2014) DLX3 regulates bone mass by targeting genes supporting osteoblast differentiation and mineral homeostasis in vivo. *Cell Death Differ.* **21**, 1365–1376
13 Singh, M., Del, C.F., Monroy, M.A., Popoff, S.N. and Safadi, F.F. (2012) Homeodomain transcription factors regulate BMP-2-induced osteoactivin transcription in osteoblasts. *J. Cell. Physiol.* **227**, 390–399
14 Hassan, M.Q., Tare, R.S., Lee, S.H., Mandeville, M., Morasso, M.I., Javed, A. et al. (2006) BMP2 commitment to the osteogenic lineage involves activation of Runx2 by DLX3 and a homeodomain transcriptional network. *J. Biol. Chem.* **281**, 40515–40526
15 Hassan, M.Q., Javed, A., Morasso, M.I., Karlin, J., Montecino, M., van Wijnen, A.J. et al. (2004) Dlx3 transcriptional regulation of osteoblast differentiation: temporal recruitment of Msx2, Dlx3, and Dlx5 homeodomain proteins to chromatin of the osteocalcin gene. *Mol. Cell. Biol.* **24**, 9248–9261
16 Ma, Y., Ma, W., Huang, L., Feng, D. and Cai, B. (2015) Long non-coding RNAs, a new important regulator of cardiovascular physiology and pathology. *Int. J. Cardiol.* **188**, 105–110
17 St, L.G., Wahlestedt, C. and Kapranov, P. (2015) The landscape of long noncoding RNA classification. *Trends Genet.* **31**, 239–251
18 Ratajczak, M.Z. (2012) Igf2-H19, an Imprinted Tandem Yin-Yanggene and its Emerging Role in Development, Proliferation of Pluripotent Stem Cells, Senescence and Cancerogenesis. *J. Stem Cell Res. Ther.* **2** (4), 108, doi:10.4172/2157-7366.1000e108
19 Ratajczak, M.Z. (2012) Igf2-H19, an imprinted tandem gene, is an important regulator of embryonic development, a guardian of proliferation of adult pluripotent stem cells, a regulator of longevity, and a 'passkey' to cancerogenesis. *Folia. Histochem. Cytobiol.* **50**, 171–179
20 Haffner, C., Frauli, M., Topp, S., Irmler, M., Hofmann, K., Regula, J.T. et al. (2004) Nicalin and its binding partner Nomo are novel Nodal signaling antagonists. *EMBO J.* **23**, 3041–3050
21 Olsen, B.R., Reginato, A.M. and Wang, W. (2000) Bone development. *Annu. Rev. Cell Dev. Biol.* **16**, 191–220
22 Merlo, G.R., Zerega, B., Paleari, L., Trombino, S., Mantero, S. and Levi, G. (2000) Multiple functions of Dlx genes. *Int. J. Dev. Biol.* **44**, 619–626
23 Morasso, M.I., Markova, N.G. and Sargent, T.D. (1996) Regulation of epidermal differentiation by a Distal-less homeodomain gene. *J. Cell Biol.* **135**, 1879–1887
24 Palazzo, E., Kellett, M., Cataisson, C., Gormley, A., Bible, P.W., Pietroni, V. et al. (2016) The homeoprotein DLX3 and tumor suppressor p53 co-regulate cell cycle progression and squamous tumor growth. *Oncogene* **35**, 3114–3124
25 Rane , S.G., Dubus, P., Mettus, R.V., Galbreath, E.J., Boden, G., Reddy, E.P. et al. (1999) Loss of Cdk4 expression causes insulin-deficient diabetes and Cdk4 activation results in beta-islet cell hyperplasia. *Nat. Genet.* **22**, 44–52
26 Connell-Crowley, L., Harper, J.W. and Goodrich, D.W. (1997) Cyclin D1/Cdk4 regulates retinoblastoma protein-mediated cell cycle arrest by site-specific phosphorylation. *Mol. Biol. Cell* **8**, 287–301
27 Serrano, M., Hannon, G.J. and Beach, D. (1993) A new regulatory motif in cell-cycle control causing specific inhibition of cyclin D/CDK4. *Nature* **366**, 704–707
28 Gao, W.L., Liu, M., Yang, Y., Yang, H., Liao, Q., Bai, Y. et al. (2012) The imprinted H19 gene regulates human placental trophoblast cell proliferation via encoding miR-675 that targets Nodal Modulator 1 (NOMO1). *RNA Biol.* **9**, 1002–1010

29 Alotaibi, M.K., Kitase, Y. and Shuler, C.F. (2016) Smad2 overexpression induces alveolar bone loss and up regulates TNF-alpha, and RANKL. *Arch. Oral. Biol.* **71**, 38–45
30 Huang, Y., Zheng, Y., Jia, L. and Li, W. (2015) Long Noncoding RNA H19 Promotes Osteoblast Differentiation Via TGF-beta1/Smad3/HDAC Signaling Pathway by Deriving miR-675. *Stem Cells* **33**, 3481–3492
31 Gabory, A., Jammes, H. and Dandolo, L. (2010) The H19 locus: role of an imprinted non-coding RNA in growth and development. *BioEssays* **32**, 473–480
32 Gabory, A., Ripoche, M.A., Le Digarcher, A., Watrin, F., Ziyyat, A., Forne, T. et al. (2009) H19 acts as a trans regulator of the imprinted gene network controlling growth in mice. *Development* **136**, 3413–3421
33 Hao, Y., Crenshaw, T., Moulton, T., Newcomb, E. and Tycko, B. (1993) Tumour-suppressor activity of H19 RNA. *Nature* **365**, 764–767
34 Davis, T.L., Yang, G.J., McCarrey, J.R. and Bartolomei, M.S. (2000) The H19 methylation imprint is erased and re-established differentially on the parental alleles during male germ cell development. *Hum. Mol. Genet.* **9**, 2885–2894
35 Nordin, M., Bergman, D., Halje, M., Engstrom, W. and Ward, A. (2014) Epigenetic regulation of the Igf2/H19 gene cluster. *Cell Prolif.* **47**, 189–199
36 Lewis, A., Lee, J.Y., Donaldson, A.V., Natanek, S.A., Vaidyanathan, S., Man, W.D. et al. (2016) Increased expression of H19/miR-675 is associated with a low fat-free mass index in patients with COPD. *J. Cachexia Sarcopenia Muscle* **7**, 330–344